

Photocatalytic degradation of Cyanobacterial Metabolites under UV-A and solar light using nanostructured photocatalyst based on reduced graphene oxide-TiO₂ composites

Theodora Fotiou^a, Theodoros M. Triantis^a, Triantafyllos Kaloudis^a, Luisa M. Pastrana-Martínez^b, Vlassis Likodimos^c, Polycarpos Falaras^c, Adrián M.T. Silva^b and Anastasia Hiskia^{a,*}

^a Laboratory of Catalytic – Photocatalytic Processes (Solar Energy – Environment), Institute of Advanced Materials, Physicochemical processes, Nanotechnology & Microsystems, National Center for Scientific Research “Demokritos”, Athens, 15310, Greece

^b LCM – Laboratory of Catalysis and Materials – Associate Laboratory LSRE/LCM, Faculdade de Engenharia, Universidade do Porto, Rua Dr. Roberto Frias, 4200-465 Porto, Portugal

^c Laboratory of Photo-redox Conversion and Storage of Solar Energy, Institute of Physical Chemistry, National Center for Scientific Research “Demokritos”, Neapoleos 25, 15310 Agia Paraskevi, Attiki, Greece

ABSTRACT

Microcystins (MCs) are natural toxins produced during cyanobacteria blooms that can occur in eutrophic waters. Microcystin-LR (MC-LR) is the most common and toxic MCs variant. Geosmin (GSM) and 2-methylisoborneol (MIB) are produced by several species of cyanobacteria and can taint water causing undesirable taste and odor. Photocatalytic degradation of MC-LR, GSM and MIB under UV-A and solar light in the presence of reduced graphene oxide-TiO₂ composite (GO-TiO₂) in aqueous solution, has been studied. Degussa P25, Kronos TiO₂ and reference TiO₂ (Ref-TiO₂) nanocatalysts were used for comparison. Under UV-A Degussa P25 found the most efficient in degradation of all target analytes followed by GO-TiO₂, Ref-TiO₂ and Kronos TiO₂. Under solar light irradiation GO-TiO₂ presented similar photocatalytic activity to Degussa P25 followed by Kronos TiO₂ and Ref-TiO₂. Intermediate products identified during photocatalytic process with GO-TiO₂ under solar light and found mainly identical to those observed by Degussa P25/UV-A. Assessment of the residual toxicity using PPIA assay in the presence of GO-TiO₂ showed that toxicity is proportional only to the remaining MC-LR in the solution. The applicability of GO-TiO₂ was evaluated under solar light in real surface water samples and found highly effective for all target analytes.

1. Introduction

The presence of cyanobacteria causes many water-quality concerns, including potential production of toxins called cyanotoxins and taste-and-odor compounds [1]. Microcystins (MCs) are the most widespread cyanotoxins that are present in diverse environments [2]. MCs in drinking water cause acute and chronic toxicity [3]. They can also cause mortality, loss of production and decrease in productivity in aquaculture and have the potential to harm consumers through the food-web, via accumulation in fresh-water fish. These are cyclic heptapeptides consisting of five invariant and two variant protein amino acids [2, 4]. About 89 MCs variants have been identified so far, with microcystin-LR (MC-LR) being the most common and most toxic variant (S1a) [5]. WHO has recommended for provisional adoption the value of 1 mg L⁻¹ as a Guideline Value for MC-LR concentration in drinking water [6].

On the other hand the most usually occurring taste-and-odor compounds produced by cyanobacterial blooms are geosmin (GSM) (S1b) and 2-methylisoborneol (MIB) (S1c) [7]. Even though they are considered non-toxic, they have strong earthy-

muddy (i.e. GSM) and musty (i.e. MIB) odors that are unacceptable by consumers [8]. These compounds also cause serious product and revenue losses in aquaculture-fisheries, through accumulation in fish-tissues that results in unacceptable off-flavours [9]. GSM and MIB odor threshold concentrations in water have been reported to be 9 and 4 µg mL⁻¹, respectively [10, 11].

In cyanobacterial bloom events, when MC-LR, GSM and MIB are released into water, treatment processes are required in order to degrade or remove these compounds. Coagulation, filtration, chlorination, ozonation, activated carbon, and certain chemical oxidation technologies have been tested to different extent for the removal of MCs from water [12, 13]. Studies have shown that GSM and MIB are generally resistant to standard water treatment, including common disinfectants and oxidants [14-16]. Previous studies have demonstrated that titanium dioxide (TiO₂) photocatalysis can effectively destroy both cyanotoxins as well as taste-and-odour compounds in aqueous solutions [17-26]. Heterogeneous TiO₂ photocatalysis has been considered as a highly promising advanced oxidation process (AOPs), which lying on the utilization of solar energy

could effectively address the ever increasing concerns for pollution abatement and water purification. The process efficiency is based on the unique capability of TiO₂ in the photo-induced generation of highly reactive chemical species upon illumination with UV light, especially hydroxyl radicals that can non-selectively attack most recalcitrant organic pollutants leading to their mineralization with no harmful end products when applied at optimum conditions [27, 28].

However, despite the high reactivity of TiO₂, the overall efficiency and its competence in solar light photocatalytic applications is essentially hampered by the relatively low quantum yield of TiO₂ i.e. the ratio of the quantity of reactant molecules consumed or the product molecules formed during the photocatalytic reaction, to the quantity of absorbed photons at a given wavelength as well as by the wide band gap of TiO₂ (3.0-3.2 eV) that allows photo-excitation only in the UV range [27-29]. Heterostructures of TiO₂ with other technologically relevant materials is considered as a promising strategy to improve photocatalytic efficiency of TiO₂ by inhibiting electron-hole recombination and enhancing its light harvesting ability by coupling with visible light absorbing materials. Among the diverse nanocomposite photocatalysts that are currently investigated [30], combination of TiO₂ with carbonaceous materials has been attracting considerable attention, due to the unique texture and adsorption capacity of carbon nanomaterials along with their advantageous optoelectronic properties [31, 32].

Graphene-based nanomaterials have recently emerged as one of the most promising candidates for the development of efficient composite photocatalysts, due to their exceptional charge carrier mobility, electrical and thermal conduction as well as large specific surface area and high transparency [33-35]. In particular, graphene oxide (GO) provide a highly functional substrate with abundant anchoring sites for efficient binding with TiO₂, whose electronic properties can be further tailored toward those of pristine graphene by judicious thermal and/or chemical reduction [36]. Intensive research efforts have been accordingly devoted to the development of tailored graphene-based-TiO₂ composite photocatalysts employing different synthetic routes that exploit GO as highly adsorptive substrate [35]. The GO-TiO₂ composite photocatalysts present systematically enhanced photocatalytic activity that is mainly related to the scavenging and subsequent transport of photo-generated electrons by GO after excitation in the conduction band of TiO₂ by UV illumination, promoting thus charge separation as well as the enhanced capacity of the composites for the physical and chemical adsorption of pollutant molecules [37]. However, performance evaluation of the GO-TiO₂ composites has been limited in most cases only to the photocatalytic degradation of dye pollutants [35]. Very recently, reduced GO-TiO₂ composite photocatalysts were prepared using the liquid phase deposition method and subsequent post-reduction upon thermal treatment in inert atmosphere [35]. These GO-TiO₂ composites outperformed the Degussa P25 catalyst for the degradation of both methyl orange azo-dye and an important pharmaceutical water pollutant (diphenhydramine) under GO loading of 3.3-4.0% wt., where optimal assembly and interfacial coupling between the reduced GO sheets and TiO₂ nanoparticles was attained.

The aim of the present study was the investigation of the photocatalytic activity of the optimized GO-TiO₂ composite photocatalyst. Commercially available Degussa P25, Kronos TiO₂ and reference-TiO₂ (Ref-TiO₂) nanocatalysts were used for comparison. Elucidation of the reaction mechanism was carried out, yst for the degradation of cyanobacterial metabolites (MC-LR, GSM and MIB) under UV-A and solar light irradiation through identification of intermediate products

formed during the photocatalytic degradation of MC-LR using GO-TiO₂ under solar light irradiation. Assessment of the residual toxicity was also performed during the course of photocatalysis.

2. Experimental

2.1. Materials

Synthesis of the GO-TiO₂ composite was performed using the liquid phase deposition method followed by post thermal treatment at 200 °C under N₂ flow as described elsewhere [35, 38]. Based on our previous studies the optimal GO loading of 4.0 % wt. in TiO₂ was used [39]. [26 fevgei] [40] The Ref-TiO₂ nanopowder was prepared using the same method but without the addition of graphene oxide, while thermal treatment has been applied under the same conditions Commercial Degussa P25 (Degussa AG, Germany) and Kronos vlp-7000, Kronos TiO₂ (Kronos Titan GmbH, Germany) were also used as standard materials for comparison purposes. MC-LR was purchased from Abraxis, USA. GSM (98.0%) and MIB (99.8%) were purchased by Wako Pure Chemical Industries Ltd. Extra pure oxygen was used for oxygenation of the solutions. Water was purified with a Millipore Milli-Q Plus System.

2.2. Instrumentation

Irradiation in UV-A ($\lambda_{\max} = 365$ nm) was performed with a laboratory constructed illumination box equipped with four F15W/T8 black light tubes (Sylvania GTE, USA), emitting 71.7 mW cm⁻² at a distance of 25 cm. Solar light was provided by an Oriel photolysis apparatus (Photomax) equipped with an Oriel 150 W Xe arc lamp, a cool water circulating liquid filter to absorb the near IR radiation and finally with an Oriel AM1.5 G air mass filter. This filter corrects the output of a 150 W xenon arc lamp to approximate the solar spectrum when the sun is at a zenith angle of 48.2 °. The light intensity was measured to be 115 mW / cm² by a power meter (Ealing Electro-Optics).

HPLC apparatus consisted of a Waters (Milford, MA, USA) Model 600E pump associated with a Waters Model 600 gradient controller, a Rheodyne (Cotati, CA, USA) Model 7725i sample injector equipped with 20 μ l sample loop, and a Waters Model 486 tunable absorbance detector, controlled by the Millennium (Waters) software.

The GC-MS system was an Agilent 6890 Series gas chromatograph interfaced to an Agilent 5973 mass selective detector.

The LC-MS/MS system was a Thermo Finnigan LC-MS /MS (San Jose, USA) consisting of a Thermo Surveyor LC pump, a Thermo Surveyor AS auto-sampler and a TSQ Quantum Discovery MAX triple quadrupole mass spectrometer equipped with an electrospray ionization (ESI) interface operating in the positive ionization mode. Xcaliber software 1.4 was used to control the mass spectrometric conditions and for data acquisition. Detection was carried out in full scan mode (300-1200 m/z). Mass axis calibration was performed by infusion of a polytyrosine-1,3,6 standard solution at 5 μ L min⁻¹. High-purity nitrogen was used as sheath and auxiliary gas and argon was used as collision gas. Sheath gas was set at 20 arbitrary units (a.u.), auxiliary gas was set at 5 a.u., and spray voltage was 5 kV. Capillary temperature was set at 350 °C and collision pressure was 1.5 mbar. Collision energy and tube lens offset were optimized for microcystin-LR.

In all cases a borosilicate glass vessel reactor was sealed and placed inside a water thermostated jacket in order to prevent evaporation and retain the sample temperature constant at 25 °C during the whole period of irradiation.

2.3. Analytical procedures

The concentration of MC-LR during the degradation process was monitored by HPLC. Acetonitrile (A) and water (B) both containing 0.05% TFA were the elution solvents. An Agilent Eclipse XDC-C18 analytical column (15 cm X 4.6 mm ID, 3.5 μm) was used and the gradient elution program was as follows: 35% A - 65% B at 0.00 min, 70% A at 2.00 min, 100% A at 2.10 min, 0% A at 3.00 min, 35% A at 3.10 min, at a flow rate of 1.2 ml/min [19]. Injection volume was 20 μl. Detection was at 238 nm. Before analysis, solutions were filtered (Millex PVDF Durapore-GF 13mm 0.22μm, low protein binding filters).

GSM and MIB were monitored by headspace solid phase micro-extraction (HS-SPME) followed by gas chromatography-mass spectrometry (GC-MS) [41]. Samples of 2 mL were placed in screw-capped headspace vials with PTFE-lined silicone septa. Sodium Chloride (750 mg) and a magnetic stirrer were added, the SPME fiber (Polydimethylsiloxane, 100 μm, Supelco) was inserted and the vial was placed for extraction at 70 °C for 30 minutes under stirring. A HP-5 MS capillary column (30 m x 0.25 mm x 0.25 mm film thickness) was used with a temperature gradient program from 50 °C (held for 1 min) to 250 °C (held for 6 min), using a temperature ramp (12 °C min⁻¹) under constant flow (1 mL min⁻¹) were used. Detection was in selected ion monitoring (SIM) mode at m/z: 112 (GSM) and 95 (MIB), respectively.

Liquid chromatography for MC-LR intermediates identification was carried out using a Kromasil 100-5C18 (5 μm, 150 mm x 2.1 mm) reversed-phase LC column. Acetonitrile (A) and high-purity water (B), both containing 0.1 % HCOOH, were the mobile phase solutions and gradient elution was programmed from 15 to 25 % of acetonitrile in 10 min, followed by an increase to 40 % in 10 min and to 80 % in the next 15 min [42]. Flow rate was set at 0.2 ml min⁻¹ and the injection volume was 50 μL, using a full loop injection. MC-LR eluted at 25.9 min.

2.4. Photocatalytic experiments

In a typical experiment for MC-LR degradation, 5ml of aqueous MC-LR solution (10 mg L⁻¹) containing 200 mg L⁻¹ of the photocatalyst (GO-TiO₂, Ref-TiO₂, commercial Degussa P25 and Kronos-TiO₂) were added to a cylindrical pyrex cell, oxygenated for twenty minutes and covered air tightly with a serum cap. Illumination was carried out at 25 °C in the photolysis apparatus.

In the case of GSM and MIB the same experimental procedure was used with the volume of aqueous solution being 20 mL, spiked with GSM or MIB to give a concentration of 1 mg L⁻¹.

Illumination was performed at ambient temperature in the illumination apparatus. The solutions were magnetically stirred throughout the experiments.

The observed rate constants were calculated from the trace of the variation of the concentration of substrates divided by their initial concentration with time for the first 30 % of the reaction (Fig. 1–6) and are roughly within 20%.

For the identification of MC-LR intermediates, a solution of 12 ml containing 10 mg L⁻¹ of MC-LR and 200 mgL⁻¹ of the photocatalyst (Degussa P25 TiO₂ and GO-TiO₂), was irradiated and samples were taken at certain times during the

process. Samples were then filtered and analyzed by LC-MS/MS.

2.4. Toxicity Measurements

Residual toxicity associated with MC-LR was assessed by the protein phosphatase inhibition assay (PPIA) using the MicroCystest kit (Zeu-Immunitec S.L., Spain) in 96-well microtiter plate format according to manufacturer's instructions. A Tecan Sunrise microplate reader was used for measurements of OD at 410 nm. Tecan Infinite M200 microplate reader (Tecan Group Ltd., Switzerland).

3. Results and Discussion

3.1. Photocatalytic degradation of MC-LR and taste-and-odor compounds by TiO₂ based nanomaterials under UV-A light

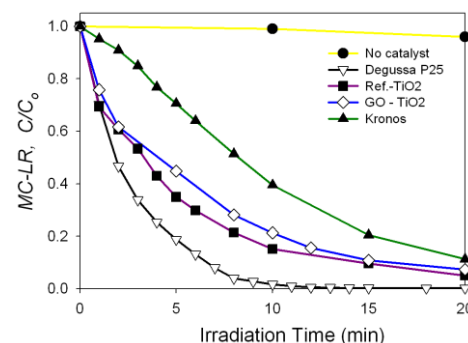


Figure 1 : Photocatalytic degradation of 10 mg L⁻¹ of MC-LR under UV-A ($\lambda_{max} = 365$ nm) irradiation in the presence of different TiO₂ based nanostructured materials, 200 mg L⁻¹ (commercial Degussa P25, Kronos-TiO₂, GO-TiO₂ and Ref-TiO₂).

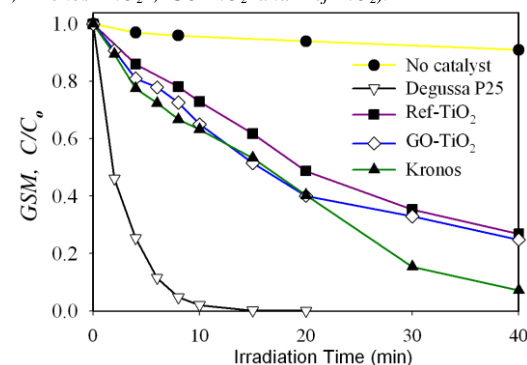


Figure 2 : Photocatalytic degradation of 1 mgL⁻¹ GSM under UV-A ($\lambda_{max} = 365$ nm) irradiation in the presence of different TiO₂ based nanostructured materials, 200 mg L⁻¹ (commercial Degussa P25, Kronos-TiO₂, GO-TiO₂ and Ref-TiO₂).

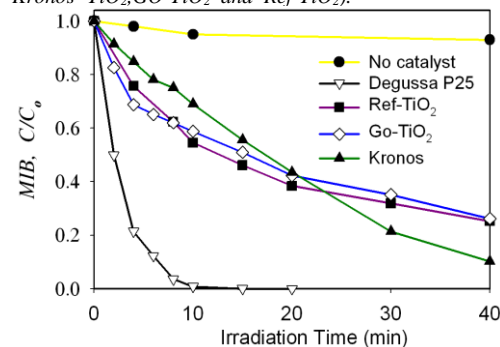


Figure 3: Photocatalytic degradation of 1 mgL⁻¹ MIB under UV-A ($\lambda_{max} = 365$ nm) irradiation in the presence of different TiO₂ based nanostructured materials, 200 mg L⁻¹ (commercial Degussa P25, Kronos-TiO₂, GO-TiO₂ and Ref-TiO₂).

Illumination of an aqueous solution of MC-LR under UV-A irradiation ($\lambda_{max} = 365$ nm) in the presence of commercial Degussa P25, Kronos-TiO₂, GO-TiO₂ and Ref-TiO₂ nanomaterials resulted in the photodegradation of the cyanotoxin (Fig. 1). Experiments performed in the absence of photocatalysts indicated that the contribution of photolysis is negligible since no degradation was observed. These results are in agreement with those reported in a previous study concerning commercial Degussa P25 [17, 19]. As can be seen in Fig. 1, Degussa P25 found the most effective in degradation of substrate followed by GO-TiO₂ and Ref-TiO₂ that exhibited similar photocatalytic performance. Kronos-TiO₂ found to be the least effective of all nanocatalysts tested. Under the experimental conditions used, observed rate constants ($k \times 10^{-3}$) were 25.1, 22.6, 23.1 and 5.9 min⁻¹ for Degussa P25, GO-TiO₂, Ref-TiO₂ and Kronos-TiO₂, respectively. In any case, after 20 min of irradiation almost complete destruction of the cyanotoxin took place by all photocatalysts, with 100% MC-LR degradation with Degussa P25, followed by Ref-TiO₂, GO-TiO₂ and Kronos-TiO₂ with 95, 94 and 89 % degradation, respectively (Fig. 1).

As far as concerning GSM and MIB, illumination under UV-A in the presence of different TiO₂ based nanostructured materials (Degussa P25, Kronos-TiO₂, GO-TiO₂ and Ref-TiO₂ nanocomposites) resulted in photodegradation of both substrates (Fig. 2 and 3, for GSM and MIB, respectively). Experiments showed that photolysis in the absence of photocatalysts is negligible. Results for Degussa P25 come in agreement with those reported in other studies [22, 25]. As can be seen in Fig. 2 and 3, under UV-A irradiation all photocatalysts were effective for destruction of GSM and MIB. Again Degussa P25 appeared to be the most effective photocatalyst in the case of both compounds with complete degradation after 20 min of irradiation. The rest of the photocatalysts showed almost the same behavior for both substrates. Destruction of GSM found 93, 75 and 73% for Kronos vlp-7000, GO-TiO₂ and Ref-TiO₂, respectively. Same for MIB, with degradation to be 90, 75 and 74% for Kronos vlp-7000, GO-TiO₂ and Ref-TiO₂, respectively. Under the experimental conditions used, the observed rate constants ($k \times 10^{-3}$) of GSM were 25, 3.4, 2.6 and 4.7 min⁻¹ for Degussa P25 TiO₂, GO-TiO₂, Ref-TiO₂ and Kronos vlp-7000, respectively. The corresponding values for MIB were 27, 5.9, 4.6 and 3 min⁻¹, respectively.

3.2. Photocatalytic degradation of MC-LR and taste-and-odor compounds by TiO₂ based nanomaterials under solar light

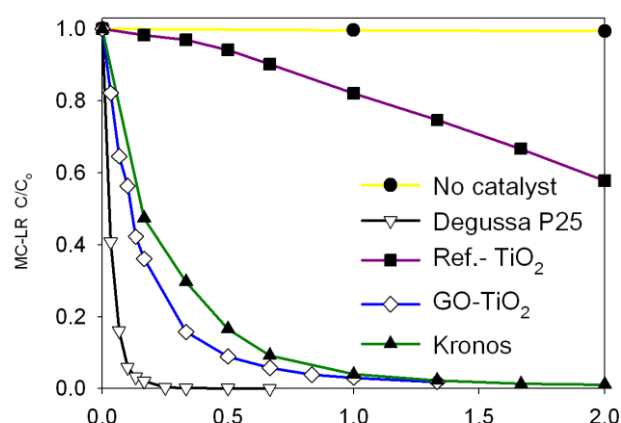


Figure 4 : Photocatalytic degradation of 10 mg L⁻¹ of MC-LR under solar light (AM 1.5 G) irradiation in the presence of different TiO₂ based nanostructured materials, 200 mg L⁻¹ (commercial Degussa P25 TiO₂, Kronos vlp-7000, GO-TiO₂ and Ref-TiO₂).

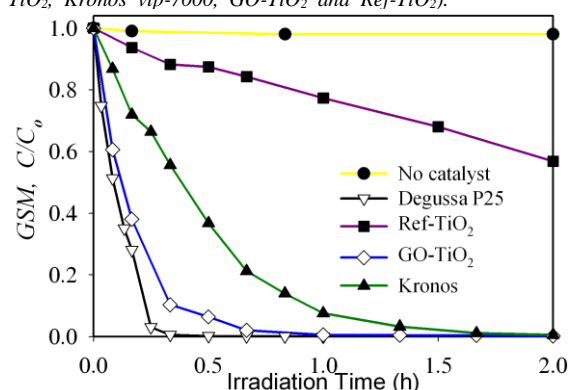


Figure 5 : Photocatalytic degradation of 1 mgL⁻¹ GSM under UV light (AM 1.5 G) irradiation in the presence of different TiO₂ based nanostructured materials, 200 mg L⁻¹ (commercial Degussa P25 TiO₂, Kronos vlp-7000, GO-TiO₂ and Ref-TiO₂).

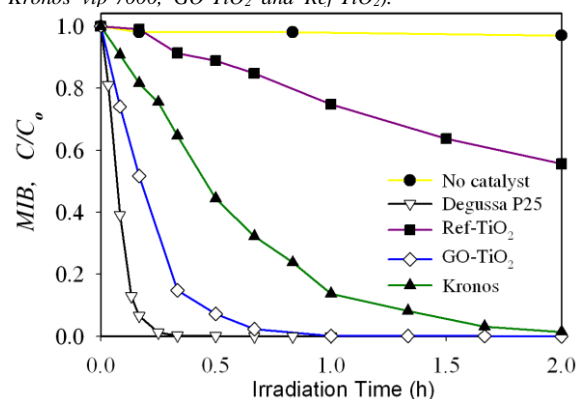


Figure 6 : Photocatalytic degradation of 1 mgL⁻¹ MIB under light (AM 1.5 G) irradiation in the presence of different TiO₂ based nanostructured materials, 200 mg L⁻¹ (commercial Degussa P25 TiO₂, Kronos vlp-7000, GO-TiO₂ and Ref-TiO₂).

As we have shown in the previous section (3.1), all tested TiO₂ based photocatalysts exhibit remarkable efficiency in photocatalytic degradation of target cyanobacterial metabolites, requiring high cost UV radiation. Activation of TiO₂ can facilitate the development of promising processes for the remediation of contaminated water resources using solar light replacing complicate facilities that generate and introduce UV light to the water.

The GO-TiO₂ photocatalyst used in this study absorbs in the whole visible region of the spectrum [39] With the band-gap narrowing attributed to the chemical bonding between

TiO₂ and the specific sites of carbon (Ti-O-C bond) [39]. Due to that, GO-TiO₂ photocatalyst has been used for the degradation of cyanobacterial metabolites under solar light irradiation. For that, the illumination apparatus employed, provided a very close spectral match to solar spectra offering significant advantages such as repeated and comparable experimental conditions and control of the local environmental parameters.

Under these experimental conditions, the GO-TiO₂ material exhibited high photocatalytic activity, similar to that of Degussa P25 TiO₂, followed by Kronos vlp-7000 and Ref-TiO₂ (Fig. 4, 5 and 6 for MC-LR, GSM and MIB, respectively). The observed rate constants ($k \times 10^{-3}$) followed the order: (i) MC-LR; Degussa P25 TiO₂ 15.3 > GO-TiO₂ 8.7 > Kronos vlp-7000 7.7 > Ref-TiO₂ 0.3 min⁻¹ ii) GSM; Degussa P25 TiO₂ 12.6 > GO-TiO₂ 10.1 > Kronos vlp-7000 2.5 > Ref-TiO₂ 0.3 min⁻¹ and (iii) MIB; Degussa P25 TiO₂ 9.6 > GO-TiO₂ 5.1 > Kronos vlp-7000 1.7 > Ref-TiO₂ 0.4 min⁻¹.

After the first hour of irradiation, Degussa P25 TiO₂ achieved complete degradation of MC-LR, followed by GO-TiO₂, Kronos TiO₂ and Ref-TiO₂ with 97, 95 and 18% degradation respectively. Correspondingly, the photocatalytic degradation of GSM, after the first hour of irradiation was 100, 99, 92 and 23% and for MIB degradation was 100, 100, 86 and 25 % for Degussa P25 TiO₂, GO-TiO₂, Kronos TiO₂ and Ref-TiO₂ respectively.

The better performance of Degussa P25 TiO₂ seems to be due to the UV part of the solar light [43].

The observed enhancement of the photocatalytic activity of GO-TiO₂ compared to Ref-TiO₂ could be attributed to the interfacial charge transfer process that can effectively inhibit electron-hole recombination as well as the enhanced capacity of the GO-TiO₂ composites for the physical and chemical adsorption of pollutant molecules [44, 45].

As far as concerning the commercial photocatalyst Kronos TiO₂, from which GO-TiO₂ was proven to be better, is a C-doped visible light activated material which is currently used for industrial purposes (i.e. air purifying paint). C-doping produces new energy states deep in the TiO₂ band gap involving substitution of oxygen by carbon atoms, which are responsible for the visible light absorption [46, 47]. For that reason it is effective in solar light which is mostly constituted by visible light.

3.3. MC-LR intermediates produced under UV-A and solar light

TiO₂ photocatalysis has been receiving increased attention for the detoxification of aquatic environment due to its high efficiency on degradation of organic pollutants. It is based on the generation of highly reactive oxygen species (e.g., HO[•]; O₂^{•-}) through the photoexcitation of the catalyst by absorbing radiation with energy equal to or greater than its band gap. The mechanism of the light induced reactions occurring on the surface of the TiO₂ has been extensively discussed [27, 28].

The assessment of pollutant disappearance is not sufficient to ensure the absence of residual products since the photocatalytic treatment is a complex procedure leading to the formation of degradation products, which in some cases may be more toxic and stable than the parent compound. Therefore careful analytical monitoring using various techniques is important in order to control all transformation steps, to identify hazardous intermediates and to clarify the reaction mechanism.

So far, a number of studies have examined degradation pathways of MC-LR applying either conventional or AOPs such as ozonation [48, 49], chlorination [50], ultra-sonication [51], photolysis [52] and even using TiO₂/UV-A [42, 53-55]. Lack of analytical standards for MC-LR reaction intermediates complicates identification of primary intermediates. In his study, identification of intermediate products formed during the photocatalytic degradation of MC-LR using GO-TiO₂ under solar light and Degussa P25 TiO₂ under UV-A was performed using LC-MS/MS. The majority of byproducts detected, appeared within the first 2 minutes of irradiation. Furthermore, the abundance of most of the byproducts initially increased but subsequently decomposed after prolonged photocatalysis. Structured assignment of intermediates produced during the course of photocatalysis MC-LR degradation was based on the analysis of the LC-MS chromatograms and the respective mass spectrum. Although many of the intermediates detected in the current study were already known [antoniou, liu], a number of new intermediates was observed (313.5, 368.5, 389, 411.5, 417, 437, 457, 515.5, 544, 781.5, 980.5 and 1031.5 m/z) and possible structures are proposed (S2).

Intermediates detected under UV-A and solar light irradiation in majority were the same, because photocatalysis under solar light is mainly due to the UV part of the spectrum. Chromatograms resulted from photocatalytic degradation of MC-LR are presented in Fig. 7a for Degussa P25 TiO₂ under UV-A irradiation (0 - 15 min) and in Fig. 7b for GO-TiO₂ under solar light irradiation (0 - 70 min). In Table 1 are presented all products observed from photocatalytic degradation of MC-LR under UV-A and solar light irradiation, retention times (R_t), molecular weight (mw) and formulas and the possible structures.

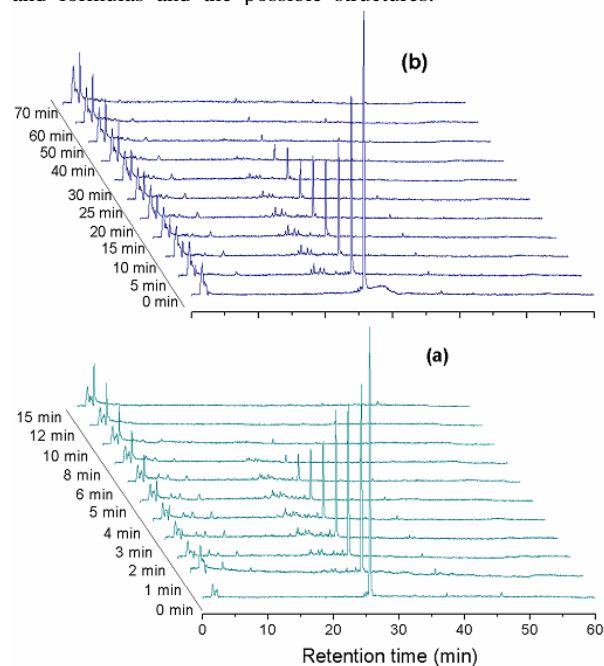


Figure 7: Chromatograms resulted from MC-LR photocatalytic degradation using a) Degussa P25 TiO₂ under UV-A irradiation and b) using GO-TiO₂ under solar light irradiation.

MC-LR is consisted by seven aminoacids, 3-amino-9-methoxy-2,6,8-trimethyl-10-phenyl-4,6-decadienoic acid (Adda), iso-glutamic acid (Glu), methyl dehydroalanine (Mdha), D-alanine (Ala), L-leucine (Leu), D-methylaspartic acid (MeAsp) and L-arginine (Arg), and it can be “written” as Cyclo[-Adda-Glu-Mdha-Ala-Leu-MeAsp-Arg-] [4]. One of the most intense peak observed (higher peak area in relative abundance)

corresponded to a product at m/z 1029 with a mass spectrum showing a molecular ion $(M + H)^+$. This product is generated by hydroxyl radical attack at either 4 or 6 double bond on the conjugated diene structure system, of the Adda chain [Adda(OH)₂], resulting in double hydroxylation of MC-LR [42, 51-53, 55]. In relative abundance chromatogram (S3), multiple peaks for 1029 m/z appeared, suggesting that except 4-5 and 6-7 dihydroxy addition, geometrical isomers of dihydroxy-MC-LR could be deduced. Further oxidation of dihydroxylated MC-LR with cleavage of the dihydroxylated bond at positions 4-5 or 6-7 on the Adda chain, results in products with m/z 795 (aldehyde intermediate) and m/z 835 (ketone intermediate), respectively. Further oxidation of product m/z 795 forms m/z 811 intermediate, consistent with a carboxylic acid structure. A new intermediate observed at m/z 1031.5 could be possibly formed from di-hydration of the double bonds of Adda [Adda(OH)₂]₂ or one hydration on Adda chain and another one on the Mdha chain [Mdha(OH)₂]. Also, m/z 1029 product could be resulted from double hydroxylation of the double bond on the chain of Mdha [Mdha(OH)₂]. Consecutive oxidation leads to the formation of an aldehyde (m/z 1011.5) [42, 51, 53] and cleavage on the C'-CO bond results the m/z 1015.5 product [53].

Another multiple peak observed was that at $m/z=1011.5$ (S3). There are different explanations concerning the pathway underwent for intermediates formed with this molecular ion. First, one consists to a hydroxyl substitution of the hydrogen at C7 to form enol-MC-LR [Adda(O)] or on the Mdha [Mdha(O)], which rapidly isomerizes to a more stable tautomer of ketone-MC-LR. The second is consisted to be a

hydroxyl substitution on aromatic hydrogen (o-, p- and to a lesser extent the m- hydroxylated product). A second hydroxylation of the aromatic ring is followed, yielding m/z 1027.5 [42, 51, 53] intermediate (explaining multiple peaks), (S3). Demethoxylated-MC-LR on the methoxy group of Adda, through the formation of the formic acid ester results in intermediate at $m/z=1009.5$ (double peak, E-Z isomers) [53], (S3). Another intermediate observed with multiple peaks at $m/z=1045.5$ [51], consists to triple hydroxylation of MC-LR (one on aromatic ring and two on Adda chain or one on aromatic ring and two on side chain of the toxin between Mdha and Ala).

The observation of intermediate with at m/z 965 ($M+Na^+$) is consistent with linearization of MC-LR, after cleavage (-C₃O) on the side chain of the toxin between Mdha and Ala [53]. After production of m/z 965, the generation of product at m/z 999.5 ($M+Na$)⁺ takes place through dihydroxylation on the Adda C6-C7 bonds [51, 55]. Further oxidation could result a to a ketone at m/z 783.5. Product at m/z 965 could also result from abstraction of the methoxy group from Adda chain [Adda(-Methoxy)]. Upon addition of amino group, a new observed product at m/z 980.5 could be formed.

Products reported in Table 1, with $m/z < 781.5$ are observed for the first time and could be oxidation products of those with higher m/z , at different sites of the molecules. For example products at 315.5, 368.5 and 411.5 m/z , could be formed after oxidation of product at m/z 1045.5.

Table 1: Products observed from MC-LR degradation using Degussa P25 TiO₂/UV-A and GO-TiO₂/solar light irradiation.

No	Peak (m/z)	Rt (min)	MW and Formula	Possible structure	Catalyst
	995.5	25.9	C ₄₉ H ₇₄ N ₁₀ O ₁₂ , 994.5	MC-LR: Cyclo [-Adda-Glu-Mdha-Ala-Leu-MeAsp-Arg-]	
1	313.5	38.1- 42.6	C ₁₆ H ₂₄ O ₆ , 312.2	Dihydroxy-7-(hydroxy-phenyl)-6-methoxy-3,5-dimethyl-heptanoic acid	TiO ₂ , GO-TiO ₂
2	368.5	21.2-25.8	C ₂₀ H ₃₃ NO ₅ , 367.2	OH-Adda(H ₂ O) ₂	GO-TiO ₂
3	389	5.3- 6.1	C ₁₅ H ₂₈ N ₆ O ₆ , 388.2	H-Arg-NHCH(OH)CH(CH ₃)CO-Glu-H	TiO ₂ , GO-TiO ₂
4	411.5	4.8, 6.4	C ₂₂ H ₃₈ N ₂ O ₅ , 410.3	OH-Adda(H ₂ O) ₂ -NHCH ₂ CH ₃	GO-TiO ₂
5	417	4.7- 6.1	C ₁₇ H ₃₂ N ₆ O ₆ , 416.2	OH-Arg-MeAsp-Leu-H	TiO ₂ , GO-TiO ₂
			C ₁₈ H ₃₂ N ₄ O ₇ , 416.2	H-MeAsp-Leu-Ala-Mdha(OH)-H	
6	437	9.1	C ₁₇ H ₃₀ N ₆ O ₆ Na, 414.2(23)	[H-Arg-NHCH(CHO)CH(CH ₃)CO-Glu-CH ₃] ⁺ Na ⁺	TiO ₂ , GO-TiO ₂
7	457	9.0	C ₂₀ H ₃₆ N ₆ O ₆ , 456.2	H ₃ C-Arg-MeAsp-Leu-COCH ₃	TiO ₂ , GO-TiO ₂
8	515.5	20.3	C ₂₁ H ₃₇ N ₇ O ₈ , 515.3	Arg-MeAsp-Leu-Ala-COOH	TiO ₂
9	544	21.5-23.8	C ₂₃ H ₄₁ N ₇ O ₈ , 543.3	Arg-MeAsp-Leu-Ala-COCHOHCH ₃	TiO ₂ , GO-TiO ₂
10	781.5	6.1	C ₃₄ H ₅₆ N ₁₀ O ₁₁ , 780.4	Cyclo[-NHCH(CH ₃)CH(CH ₃)CO-Glu-Mdha-Ala-Leu-MeAsp-Arg-]	TiO ₂ , GO-TiO ₂
11	783.5	5.1	C ₃₃ H ₅₄ N ₁₀ O ₁₂ , 782.4	Cyclo[-NHCHOHCH(CH ₃)CO-Glu-Mdha-Ala-Leu-MeAsp-Arg-]	TiO ₂ , GO-TiO ₂
12	795	4.8-6.1	C ₃₄ H ₅₄ N ₁₀ O ₁₂ , 794.4	Cyclo[-NHCH(CHO)CH(CH ₃)CO-Glu-Mdha-Ala-Leu-MeAsp-Arg-]	TiO ₂ , GO-TiO ₂
13	811.5	4.8	C ₃₄ H ₅₄ N ₁₀ O ₁₃ , 810.4	Cyclo[-NHCH(COOH)CH(CH ₃)CO-Glu-Mdha-Ala-Leu-MeAsp-Arg-]	TiO ₂
14	835.5	9.1	C ₃₇ H ₅₈ N ₁₀ O ₁₂ , 834.4	Cyclo[-NHCH(CHCHCOCH ₃)CH(CH ₃)CO-Glu-Mdha-Ala-Leu-MeAsp-Arg-]	TiO ₂ , GO-TiO ₂
15	837.5	6.2, 9.0	C ₃₆ H ₅₆ N ₁₀ O ₁₃ , 836.4	Cyclo[-NHCH(CHCHCOOH)CH(CH ₃)CO-Glu-Mdha-Ala-Leu-MeAsp-Arg-]	TiO ₂
16	965	28.7	C ₄₈ H ₇₂ N ₁₀ O ₁₁ , 964.5	Cyclo[-Adda(□Methoxy)-Glu-Mdha-Ala-Leu-MeAsp-Arg-]	TiO ₂ , GO-TiO ₂
			C ₄₆ H ₇₄ N ₁₀ O ₁₁ Na, 942.5(23)	[H ₃ CNH-Glu-Adda-Arg-MeAsp-Leu- Ala-H] ⁺ Na ⁺	
17	980.5	26.0	C ₄₈ H ₇₅ N ₁₁ O ₁₁ , 979.5	Cyclo[-Adda(H ₂ N)(□Methoxy)-Glu-Mdha-Ala-Leu-MeAsp-Arg-]	GO-TiO ₂
18	999.5	26.2	C ₄₈ H ₇₄ N ₁₀ O ₁₃ , 998.5	Cyclo[-Adda-Glu(□Carboxy)-Mdha-Ala-Leu-MeAsp-Arg-]	TiO ₂ , GO-TiO ₂
19	1009.5	24.0-25.2	C ₄₉ H ₇₂ N ₁₀ O ₁₃ , 1008.5	Cyclo[-DmAdda-Glu-Mdha-Ala-Leu-MeAsp-Arg-]	TiO ₂ , GO-TiO ₂
20	1011.5	21.4-25.7	C ₄₉ H ₇₄ N ₁₀ O ₁₃ , 1010.5	(OH)-Cyclo[-Adda-Glu-Mdha-Ala-Leu-MeAsp-Arg-] Cyclo[-Adda(O)-Glu-Mdha-Ala-Leu-MeAsp-Arg-] Cyclo[-Adda-Glu-Mdha(O)-Ala-Leu-MeAsp-Arg-]	TiO ₂ , GO-TiO ₂
21	1015.5	26.0	C ₄₈ H ₇₄ N ₁₀ O ₁₄ , 1014.5	(CO)Ala-Leu-MeAsp-Arg-Adda-Glu(NCOCH ₃)	TiO ₂ , GO-TiO ₂

No	Peak (m/z)	Rt (min)	MW and Formula	Possible structure	Catalyst
22	1027.5	22.6-26.4	C ₄₉ H ₇₄ N ₁₀ O ₁₄ , 1026.5	(OH) ₂ -Cyclo[-Adda-Glu-Mdha-Ala-Leu-MeAsp-Arg-]	TiO ₂ , GO-TiO ₂
23	1029	20.3-22.1	C ₄₉ H ₇₆ N ₁₀ O ₁₄ , 1028.6	Cyclo[-Adda(OH) ₂ -Glu-Mdha-Ala-Leu-MeAsp-Arg-] Cyclo[-Adda-Glu-Mdha(OH) ₂ -Ala-Leu-MeAsp-Arg-]	TiO ₂ , GO-TiO ₂
24	1031.5	21.9	C ₄₉ H ₇₈ N ₁₀ O ₁₄ , 1030.6	Cyclo[-Adda(OH) ₂ -Glu-Mdha-Ala-Leu-MeAsp-Arg-] Cyclo[-Adda(OH) ₂ -Glu-Mdha(OH) ₂ -Ala-Leu-MeAsp-Arg-]	TiO ₂ , GO-TiO ₂
25	1045.5	20-27	C ₄₇ H ₇₇ N ₁₀ O ₁₅ , 1044.6	OH-Cyclo[-Adda(OH) ₂ -Glu-Mdha-Ala-Leu-MeAsp-Arg-] OH-Cyclo[-Adda-Glu-Mdha(OH) ₂ -Ala-Leu-MeAsp-Arg-]	TiO ₂

3.4. Toxicity assessment

As far as drinking water treatment is concerned for the recovery of water after contamination with MC-LR or other microcystins, an important question is raised: At what stage of treatment the water becomes detoxified? In other words, is degradation of the initial compound sufficient to remove the toxic activity, or complete mineralization is needed? The answer to this question is of major importance not only for water safety but also for the efficiency and cost-effectiveness of the treatment process, especially when intended for use in large-scale. In an attempt to answer this, the residual toxicity of water during the course of the photocatalytic degradation of MC-LR was studied using the protein phosphatase inhibition assay (PPIA).

PPIA was developed on the basis of the ability of MCs to inhibit serine and threonine phosphatase enzymes (An & Carmichael, 1994). The extent of inhibition of these enzymes is associated to hepatotoxicity and tumor promotion. The PPIA colorimetric assay is fast and easy to use and provides important toxicological information regarding the bioactivity of MCs, since detection is based on functional activity rather than on recognition of chemical structure.

PPIA measurements that were carried out using two photocatalysts (GO-TiO₂ and Degussa P25) showed that residual toxicity was directly proportional only to the amount of MC-LR that remained intact into solution. Reduction of MC-LR concentration resulted in reduction of a directly proportional amount of the toxic activity. Moreover, in solutions that MC-LR was completely degraded, no toxic activity was observed, even though those solutions contained oxidation by-products. This implies that MC-LR loses its toxic activity (protein phosphatase inhibition) as soon as the molecule is transformed to oxidized products. This is in agreement with previously reported studies [22] where it was shown that hydroxyl radical attack on the Adda amino acid of MC-LR is the first oxidation step and results in loss of toxic activity. This finding is very important for real applications of the photocatalytic process, since it denotes that the target of the process could be degradation rather than mineralization, and therefore less energy is needed for the detoxification of water.

3.5. Application in real water samples

In order to evaluate the GO-TiO₂ nanocomposite photocatalytic performance when natural constituents of water are present, experiments in natural surface water were carried out, using solar light irradiation. Surface waters that were collected from two lakes of in Greece that also serve as water reservoirs for the population of Athens, i.e. Mornos Lake and Marathonas Lake were used as natural matrices. The basic physicochemical parameters of these waters are shown in Table 2. Water samples were spiked with known

concentrations of MC-LR, MIB and GSM at concentrations of 10 mg L⁻¹, 1 mg L⁻¹ and 1 mg L⁻¹ respectively.

Table 2 : Physicochemical parameters of surface water samples (before spiking)

Test	Marathonas Lake	Mornos Lake
pH	8.2	8.1
Dissolved Org. Carbon (mgL ⁻¹)	2.5	1.4
Total Alkalinity (mg CaCO ₃ L ⁻¹)	123	132
Conductivity (mS)	386	304
Total Hardness (mg L ⁻¹)	169	145
Turbidity (NTU)	1.7	1.5

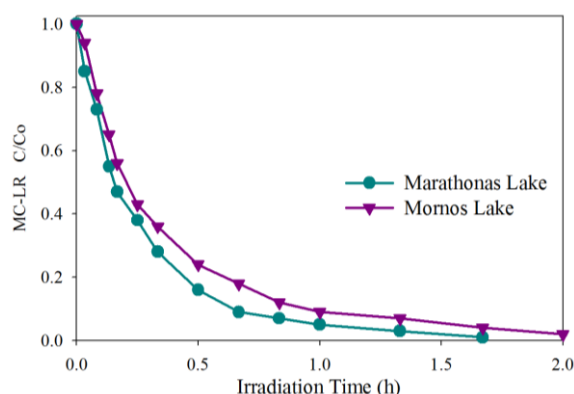


Figure 8 : Photocatalytic degradation of MC-LR (10 mgL⁻¹) under solar light irradiation, using GO-TiO₂ photocatalyst (200 mgL⁻¹) in real water samples.

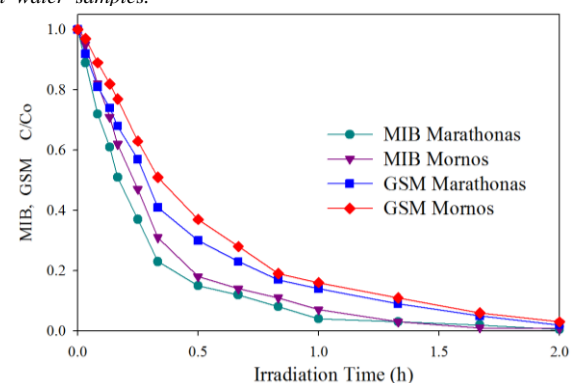


Figure 9 : Photocatalytic degradation of MIB and GSM (1 mgL⁻¹) under solar light irradiation, using GO-TiO₂ photocatalyst (200 mgL⁻¹) in real water samples.

Irradiation of samples was carried out with solar light and GO-TiO₂ (200 mgL⁻¹) was used as the photocatalyst. As shown in Fig. 8 and 9, all pollutants were successively removed from spiked natural water solutions, similarly to the experiments that were carried out in ultrapure water. The observed rate constants ($k \times 10^{-3}$) for MC-LR, GSM and MIB were respectively, 5.3, 3.2 and 5.7 min⁻¹ for Marathonas

lake, and 4.5, 2.3 and 3.7 min⁻¹, respectively for Mornos lake, respectively. These results show that GO-TiO₂ remains an effective photocatalyst even in natural waters which contain natural organic matter and other constituents that may compete with the target pollutants for the reactive oxidative species produced by the photocatalytic process. The results are promising for up-scaling of the process for natural water detoxification/decontamination (e.g. fisheries-aquaculture) as well as for drinking water treatment.

Conclusions

In this work the photocatalytic efficiency of synthesized GO-TiO₂ was evaluated for the degradation of the hepatotoxic MC-LR and the odorous compounds GSM and MIB.

Under UV-A Degussa P25 TiO₂ found to be the most efficient in degradation of all target analytes followed by GO-TiO₂, Ref-TiO₂ and Kronos TiO₂, that exhibited similar photocatalytic performance for GSM and MIB. In the case of MC-LR Kronos TiO₂ was found to have the lowest activity. Under solar light irradiation GO-TiO₂ presented similar photocatalytic activity to Degussa P25 TiO₂ followed by Kronos TiO₂ and Ref-TiO₂.

Furthermore, identification of the intermediate products formed during the photocatalytic degradation of MC-LR was achieved using the GO-TiO₂ nanocatalyst under solar light irradiation. They were found mainly identical to those observed by Degussa P25 TiO₂ under UV-A, suggesting that photodegradation mechanism takes place via a common reagent, i.e. hydroxyl radicals. Assessment of the residual toxicity of MC-LR during the course of degradation using PPIA assay under UV-A and solar light irradiation showed that toxicity is proportional only to the remaining MC-LR in the solution; therefore degradation products present no significant protein phosphatase inhibition activity. In addition, experiments performed using surface water samples have shown that GO-TiO₂ is almost as effective as in the case of using deionised water spiked with the three target compounds.

Based on the results we can conclude that GO-TiO₂ can effectively degrade MIB and GSM as well as the toxin MC-LR eliminating its toxicity and it can be further applied in lab and pilot-plant scale photoreactors.

5. Acknowledgments

This work was funded by the European Commission (Clean Water – Grant Agreement Number 227017). Clean Water is a Collaborative Project co-funded by the Research DG of the European Commission within the joint RTD activities of the Environment and NMP Thematic Priorities. T. Triantis and T. Fotiou are grateful to NCSR Demokritos, Institute of Advanced Materials, Physicochemical processes, Nanotechnology & Microsystems, for postdoctoral and PhD fellowships.

References

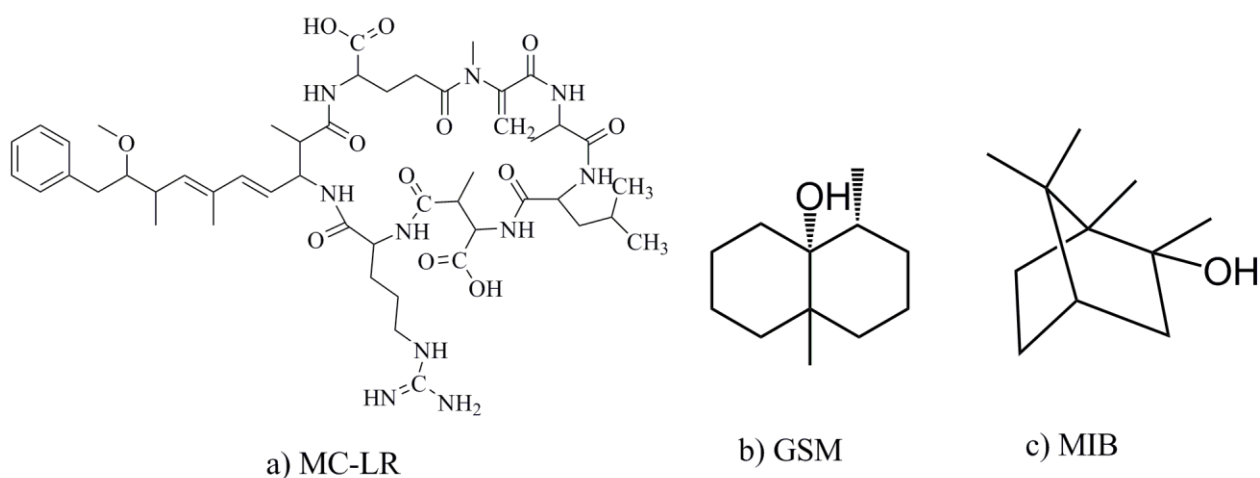
[1] W. W. Carmichael, *Sci. Am.* 270 (1994) 78-86.
 [2] K. Sivonen, G. Jones, (Eds), i. I. C. a. J. B., *Cyanobacterial toxins. In Toxic cyanobacteria in water: a guide to their public health*

consequences, monitoring, and management, E & FN Spon, New York, 1999, 41-111.
 [3] W.W. Carmichael, *Adv. Bot. Res.* 27 (1997) 211-256.
 [4] D.P. Botes, P.L. Wessels, H. Kruger, M.T.C. Runnegar, S. Santikarn, R.J. Smith, J.C.J. Barna, D.H. Williams, *J. Chem. Soc., Perkin Trans. 1* (1985) 2747-2748.
 [5] R.M. Dawson, *Toxicol.* 36 (1998) 953-962.
 [6] WHO, *Cyanobacterial toxins: microcystin-LR. Guidelines for Drinking-Water Quality*, World Health Organization, Geneva, 1998 pp. 95-110.
 [7] G.A. Burlingame, R.M. Dann, G.L. Brock, *J. Am. Water Works Assoc.* 78 (1986) 56-61.
 [8] M. J. McGuire, *Water Sci. Technol.* 31 (1995) 1-8.
 [9] Z. G. Papp, É. Kerepeczki, F. Pekár, D. Gál, *Water Sci. Technol.* 55 (2007) 301-309.
 [10] I.H. Suffett, A. Corado, D. Chou, M.J.M. McGuire, S. Butterworth, *J. Am. Water Works Assoc.* 88 (1996) 168-180.
 [11] Rashash D. M. C., A. M. Dietrich, R. C. Hoehn, *J. Am. Water Works Assoc.* 89 (1997) 131-141.
 [12] L. A. Lawton, P. K. J. Robertson, *Chem. Soc. Rev.* 28 (1999) 217-224.
 [13] V. K. Sharma, T. M. Triantis, M. G. Antoniou, X. He, M. Pelaez, C. Han, W. Song, K. E. O'Shea, A. A. De la Cruz, T. Kaloudis, A. Hiskia, D. D. Dionysiou, *Sep. Purif. Technol.* 91 (2012) 3-17.
 [14] D. Bruce, P. Westerhoff, A. Brawley-Chesworth, *J. Water Supply Res. T.* 51 (2002) 183-197.
 [15] S. Lalezary, M. Pirbazari, M. J. McGuire, *J. Am. Water Works Assoc.* 78 (1986) 62-69.
 [16] W.H. Glaze, S. Raymond, W. Chauncey, R.C. Edward, J.J. Zarnoch, E.M. Aieta, C.H. Tate, M.J. McGuire, *J. Am. Water Works Assoc.* 82 (1990) 79-84.
 [17] P. K. J. Robertson, L. A. Lawton, B. Münch, J. Rouzade, *Chem. Commun.* (1997) 393-394.
 [18] P.K.J. Robertson L. A. L., B. Munch, B.J.P.A. Cornish, *J. Adv. Oxid. Technol.* 4 (1999) 20-26.
 [19] T. M. Triantis, T. Fotiou, T. Kaloudis, A. G. Kontos, P. Falaras, D. D. Dionysiou, M. Pelaez, A. Hiskia, *Journal of hazardous materials* 211-212 (2012) 196-202.
 [20] L. A. Lawton, P. K. J. Robertson, B. J. P. Cornish, M. Jaspars, *Environ. Sci. Technol.* 33 (1999) 771-775.
 [21] X. Feng, F. Rong, D. Fu, C. Yuan, Y. Hu, *Chin. Sci. Bull.* 51 (2006) 1191-1198.
 [22] L. Lawton, P.K.J. Robertson, D. Bruce, *Appl. Catal., B* 44 (2003) 9-13.
 [23] E. Bellu, L.A. Lawton, P.K.J. Robertson, *J. Adv. Oxid. Technol.* 11 (2008) 384-388.
 [24] E. E. Bamuzza Pemu, E.M. Chirwa, *Chem. Eng. Trans.* 24 (2011) 91.
 [25] T. Fotiou, T.M. Triantis, T. Kaloudis, E. Papaconstantinou, A. Hiskia, submitted for publication (2013)
 [26] H. Choi, M. G. Antoniou, M. Pelaez, A. A. De La Cruz, J. A. Shoemaker, D. D. Dionysiou, *Environ. Sci. Technol.* 41 (2007) 7530-7535.
 [27] M. R. Hoffmann, S. T. Martin, W. Choi, D. W. Bahnemann, *Chem. Rev.* 95 (1995) 69-96.
 [28] P. Pichat, *Water Sci. Technol.* 55 (2007) 167-173.
 [29] A. Kubacka A., M. Fernandez Garcia, G. Colon, *Chem. Rev.* 112 (2012) 1555-1614.
 [30] G. Liu, L. Wang, H.G. Yang, H.M. Cheng, Q.M. Gao, G. Lu, *J. Mater. Chem.* 20 (2010) 831-843.
 [31] K. Woan, G. Pyrgiotakis, W. Sigmund, *Adv. Mater.* 21 (2009) 2233-2239.
 [32] R. Leary, A. Westwood, *Carbon* 49 (2011) 741-772.
 [33] Q. Xiang, J. Yu, M. Jaroniec, *Chem. Soc. Rev.* 41 (2012) 782-796.
 [34] X. An, J. C. Yu, *RSC Advances* 1 (2011) 1426-1434.
 [35] S. Morales-Torres, L.M. Pastrana-Martinez, J.L. Figueiredo, J.L. Faria, A.M. Silva, *Environ. Sci. Pollut. Res. Int.* 19 (2012) 3676-3687.
 [36] K.P. Loh, Q. Bao, G. Eda, M. Chhowalla, *Nat. Chem.* 2 (2010) 1015-1024.
 [37] G. Williams, B. Seger, P.V. Kamat, *ACS Nano* 2 (2008) 1487-1491.
 [38] G. Jiang, Z. Lin, C. Chen, L. Zhu, Q. Chang, N. Wang, W. Wei, H. Tang, *Carbon* 49 (2011) 2693-2701.
 [39] L.M. Pastrana-Martínez, S. Morales-Torres, V. Likodimos, J.L. Figueiredo, J.L. Faria, P. Falaras, A.M.T. Silva, *Appl. Catal., B* 123-124 (2012) 241-256.

- [40] S. Stankovich, D.A. Dikin, R.D. Piner, K.A. Kohlhaas, A. Kleinhammes, Y. Jia, Y. Wu, S.T. Nguyen, R.S. Ruoff, *Carbon* 45 (2007) 1558-1565.
- [41] K. Saito, K. Okamura, H. Kataoka, *J. Chromatogr. A* 1186 (2008) 434-437.
- [42] M.G. Antoniou, A.A. De La Cruz, D.D. Dionysiou, *Environ. Sci. Technol.* 44 (2010) 7238-7244.
- [43] D. C. Hurum, A. G. Agrios, K. A. Gray, T. Rajh, M. C. Thurnauer, *J. Phys. Chem. B* 107 (2003) 4545-4549.
- [44] H. Zhang, X. Lv, Y. Li, Y. Wang, J. Li, *ACS Nano* 4 (2009) 380-386.
- [45] Y. Zhang, Z. R. Tang, X. Fu, Y. J. Xu, *ACS Nano* 4 (2010) 7303-7314.
- [46] S. Goldstein, D. Behar, J. Rabani, *J. Phys. Chem. C* 112 (2008) 15134-15139.
- [47] S. Goldstein, D. Behar, J. Rabani, *J. Phys. Chem. C* 113 (2009) 12489-12494.
- [48] H.F. Miao, F. Qin, G.J. Tao, W.Y. Tao, W.Q. Ruan, *Chemosphere* 79 (2010) 355-361.
- [49] F.A. Al Momani, N. Jarrah, *J. Environ. Sci. Health A Tox. Hazard Subst. Environ. Eng.* 45 (2010) 719-731.
- [50] T. P. J. Kull, P. H. Backlund, K. M. Karlsson, J. A. O Meriluoto, *Environ. Sci. Technol.* 38 (2004) 6025-6031.
- [51] W. Song, A.A. de la Cruz, K. Rein, K.E. O'Shea, *Environ. Sci. Technol.* 40 (2006) 3941-3946.
- [52] K. Tsuji, S. Naito, F. Kondo, N. Ishikawa, M.F. Watanabe, M. Suzuki, K. Harada, *Environ. Sci. Technol.* 28 (1994) 173-177.
- [53] M. G. Antoniou, J. A. Shoemaker, A. A. de la Cruz, D. D. Dionysiou, *Toxicol.* 51 (2008) 1103-1118.
- [54] H. Choi, M. G. Antoniou, M. Pelaez, A. A. De La Cruz, J. A. Shoemaker, D. D. Dionysiou, *Environ. Sci. Technol.* 41 (2007) 7530-7535.
- [55] I. Liu, L. A. Lawton, P. K. J. Robertson, *Environ. Sci. Technol.* 37 (2003) 3214-3219.

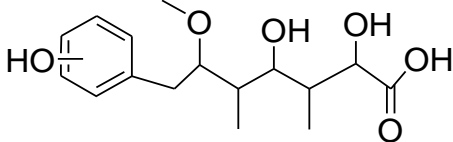
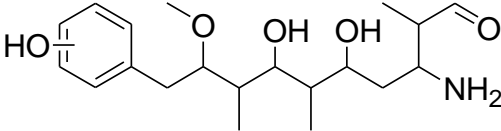
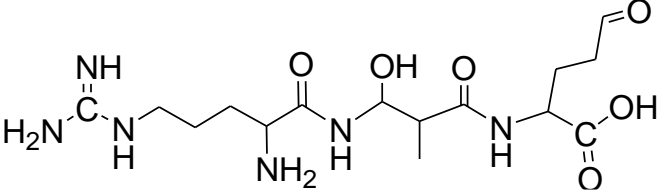
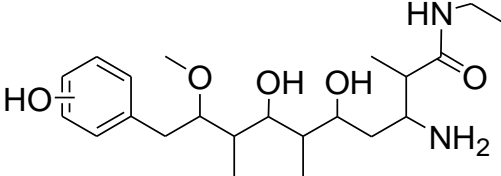
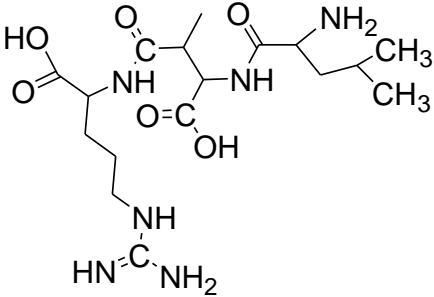
Supporting Material

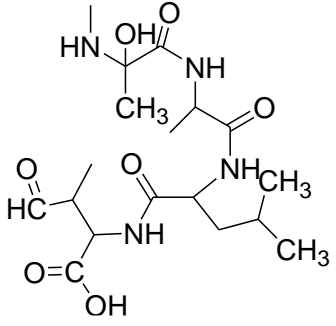
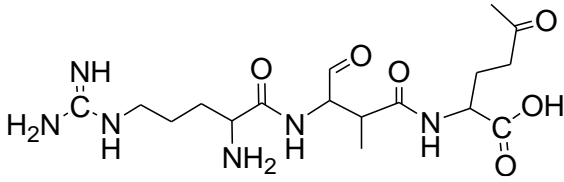
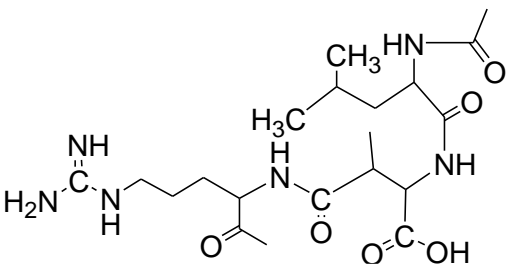
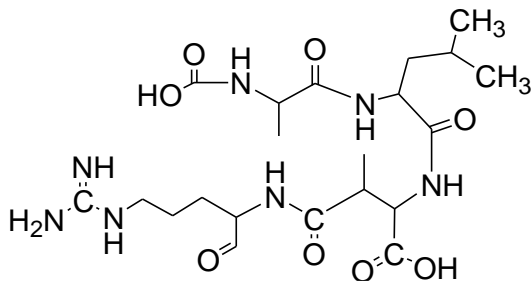
S1: Structures of a) MC-LR, b) GSM and c) MIB.

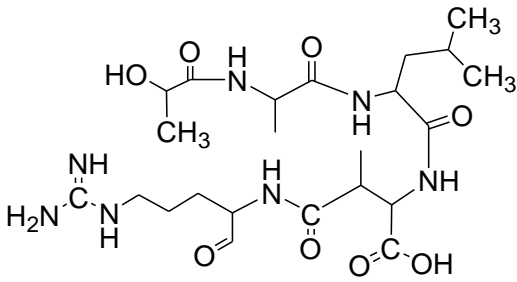
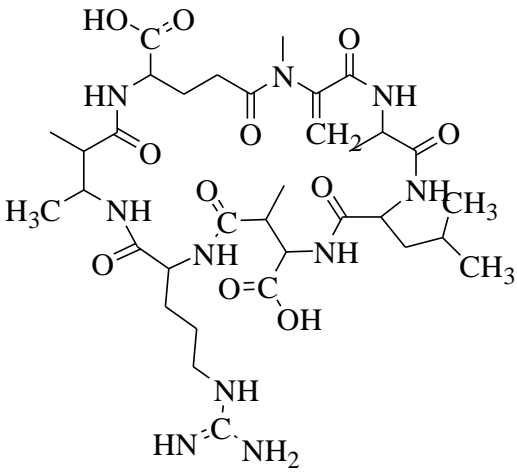
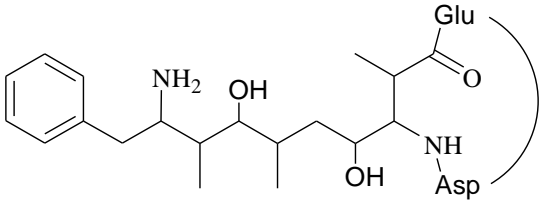


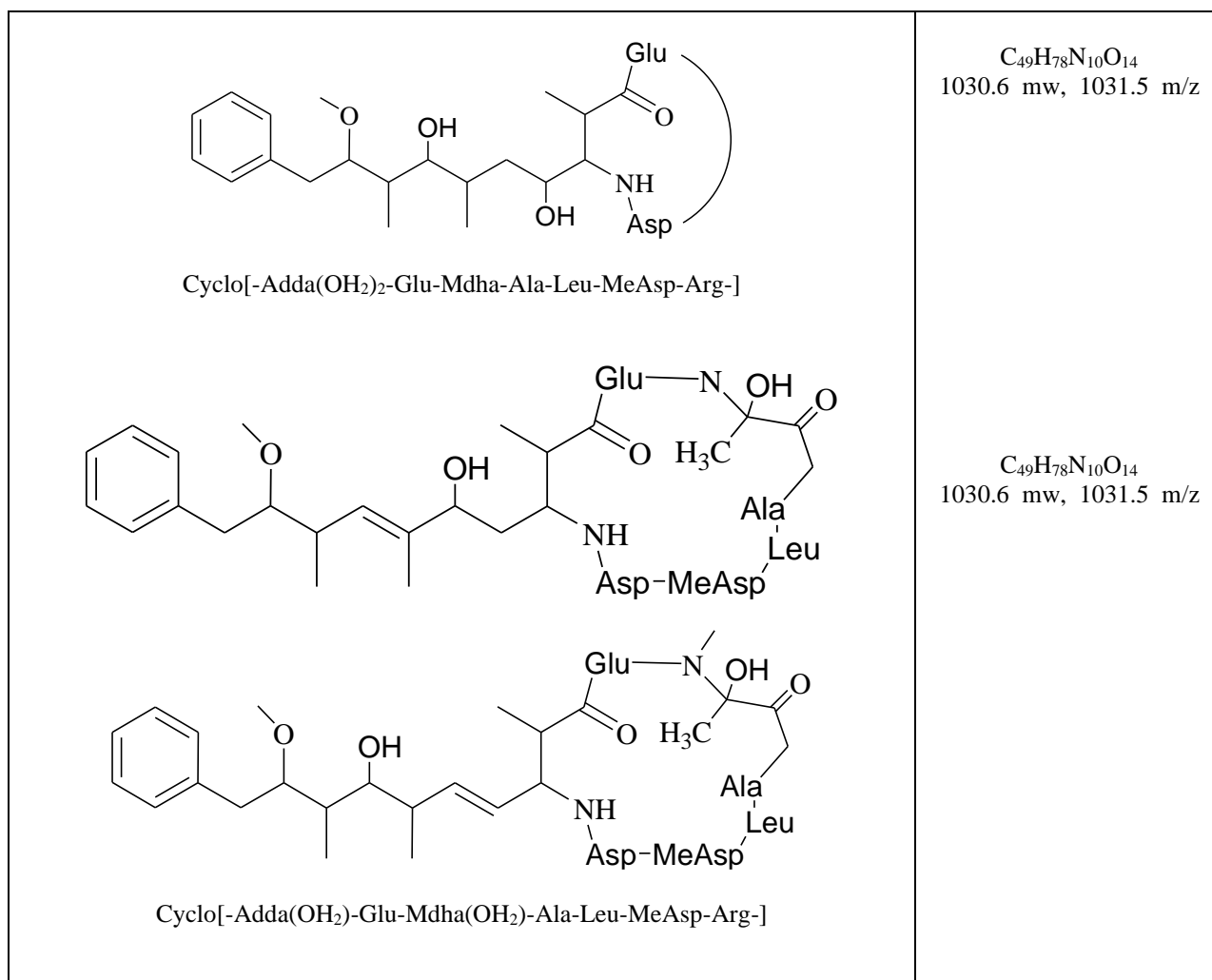
S2: Table: New intermediates observed from MC-LR

Proposed Structure	Formula, Molecular Weight, m/z
--------------------	--------------------------------

 <p>Dihydroxy-7-(hydroxy-phenyl)- 6-methoxy-3,5-dimethyl-heptanoic acid</p>	<p>$C_{16}H_{24}O_6$ 312.2 mw, 313.5 m/z</p>
 <p>OH-Adda(H₂O)₂</p>	<p>$C_{20}H_{33}NO_5$ 367.2 mw, 368.5 m/z</p>
 <p>H-Arg-NHCH(OH)CH(CH₃)CO-Glu-H</p>	<p>$C_{15}H_{28}N_6O_6$ 388.2 mw, 389.5 m/z</p>
 <p>OH-Adda(H₂O)₂-NHCH₂CH₃</p>	<p>$C_{22}H_{38}N_2O_5$ 410.3 mw, 411.5 m/z</p>
 <p>OH-Arg-MeAsp-Leu-H</p>	<p>$C_{17}H_{32}N_6O_6$ 416.2mw, 417 m/z</p>

 <p>H-MeAsp-Leu-Ala-Mdha(OH)-H</p>	<p>$C_{18}H_{32}N_4O_7$ 416.2mw, 417 m/z</p>
 <p>H-Arg-NHCH(CHO)CH(CH₃)CO-Glu-CH₃]Na⁺</p>	<p>$C_{17}H_{30}N_6O_6Na$ 414.2 (+23) mw, 437 m/z</p>
 <p>H₃C-Arg-MeAsp-Leu-COCH₃</p>	<p>$C_{20}H_{36}N_6O_6$ 456.2 mw, 457 m/z</p>
 <p>Arg-MeAsp-Leu-Ala-COOH</p>	<p>$C_{21}H_{37}N_7O_8$ 515.3 mw, 515.5 m/z</p>

 <p>Arg-MeAsp-Leu-Ala-COCHOHCH₃</p>	<p>C₂₃H₄₁N₇O₈ 543.3 mw, 544 m/z</p>
 <p>Cyclo[-NHCH(CH₃)CH(CH₃)CO-Glu-Mdha-Ala-Leu-MeAsp-Arg-]</p>	<p>C₃₄H₅₆N₁₀O₁₁ 780.4 mw, 781.5 m/z</p>
 <p>Cyclo[-Adda(H₂N)(-Methoxy)-Glu-Mdha-Ala-Leu-MeAsp-Arg-]</p>	<p>C₄₈H₇₅N₁₁O₁₁ 979.5 mw, 980.5 m/z</p>



S3: LC-MS chromatograms of MC-LR photocatalytic degradation after 5 min of irradiation under UV-A using Degussa P25 TiO₂.

